III - 50

PREPRINT NO. 77-LC-3A-2
ASLE PREPRINT

Stiffness and Damping Coefficients for the Five-Pad Tilting-Pad Bearing

J. C. NICHOLAS, E. J. GUNTER, and P. E. ALLAIRE
University of Virginia
Charlottesville, Virginia 22901

Stiffness and damping coefficients are presented for the 5-pad tilt-pad bearing for various preloads, offsets, length to diameter ratios and pad loadings (on and between pad). Finite elements and the pad assembly method are used to calculate these coefficients and the effects of the unloaded pads are included. Design curves suitable for tilt-pad bearings in widespread industrial use are presented.

Presented as an American Society of Lubrication Engineers paper at the ASLE/ASME Lubrication Conference in Kansas City, Missouri, October 3-5, 1977

INTRODUCTION

It has been known for many years that fluid film bearings such as the plain journal bearing can cause oil whirl instability in turbomachinery (*1*)-(*3*). The tilt-pad bearing has virtually eliminated oil whirl instability (*4*) (*5*) and has increased

NOMENCLATURE

c_b = $R_v - R$, tilt-pad bearing assembled radial clearance in line with a pivot (L)
c_p = $R_p - R$, pad radial clearance (L)
C_{xx}, C_{yy} = horizontal, vertical bearing damping (FTL^{-1})
$\overline{C}_{xx}, \overline{C}_{yy}$ = $C_{xx}\ (\omega_j c_P/W_T)$, $C_{yy}(\omega_j c_P/W_T)$, horizontal, vertical dimensionless damping coefficients
$\overline{C}_{\eta\eta}, \overline{C}_{\eta\xi}, \overline{C}_{\xi\eta}, \overline{C}_{\xi\xi}$ = dimensionless fixed pad damping coefficients
$\overline{C}'_{\xi\xi}$ = dimensionless dynamic pad damping coefficient
D = journal diameter (L)
e_b = bearing eccentricity (L)
h_p = pivot film thickness (L)
$\overline{h}_p, \overline{h}_{p_i}$ = h_p/c_p, dimensionless pivot film thickness, pivot film thickness for i^{th} pad
K_{xx}, K_{yy} = horizontal, vertical bearing stiffness (FL^{-1})

$$\overline{K}_{xx}, \overline{K}_{yy} = K_{xx}\left(\frac{c_P}{W_T}\right), \quad K_{yy}\ 8\left(\frac{c_P}{W_T}\right) \text{ horizontal,}$$

vertical dimensionless stiffness coefficients
$\overline{K}_{\eta\eta}, \overline{K}_{\eta\xi}, \overline{K}_{\xi\eta}, \overline{K}_{\xi\xi}$ = dimensionless fixed pad stiffness coefficients
$\overline{K}'_{\xi\xi}$ = dimensionless dynamic pad stiffness coefficient
L = bearing length (L)
m_b = $1 - (c_b/c_p)$, bearing preload factor
n_p = number of pads
N_s = shaft rotational speed (RPS)
$0_b, 0_j, 0_p$ = bearing, journal, pad center

$$p = \frac{\overline{K}_{\eta\eta}}{\overline{K}^2_{\eta\eta} + \overline{C}^2_{\eta\eta}}$$

$$q = \frac{\overline{C}_{\eta\eta}}{\overline{K}^2_{\eta\eta} + \overline{C}^2_{\eta\eta}}$$

R, R_c = journal radius, radius from bearing center to pivot (L)
R_p = pad radius of curvature (L)

$$S = \frac{\mu N_s L D}{W_T}\left(\frac{R}{c_p}\right)^2, \quad \text{Sommerfeld number}$$

S_i^{-1} = dimensionless load for the i^{th} pad
W_T = bearing external load (F)
$\overline{W}_x, \overline{W}_y$ = dimensionless horizontal, vertical hydrodynamic load
$\overline{W}_{x_i}, \overline{W}_{y_i}$ = dimensionless horizontal, vertical hydrodynamic load for the i^{th} pad
X, Y = coordinate system for tilt-pad bearing
α = θ_p/χ, bearing offset factor
ϵ_b, ϵ_p = $e_b/c_b, e_b/c_p$, eccentricity ratio
η, ξ = fixed pad coordinate system
θ_p = angle from leading edge of pad to pad pivot point (degrees)
μ = average fluid viscosity (FT/L^2)
ϕ, ϕ_i = angle from positive X-axis to pad, i^{th} pad pivot point measured in direction of rotation (degrees)
χ = pad arc length (degrees)
Ψ = attitude angle measured with rotation from the static load vector (negative Y-axis) to the eccentricity vector
ω_j = shaft rotational speed counterclockwise (T^{-1})

the maximum operating speed of rotor-bearing systems from around 6000 rpm to 10 000 or even 14 000 rpm. At these higher speeds, other destabilizing factors contribute to machine instability, such as aerodynamic cross coupling (6)-(9) and internal friction (8)-(14). The proper choice of tilt-pad bearings is essential to control these instabilities. This choice is difficult because there are many geometric variables available in tilt-pad bearing design, such as the bearing clearance, offset factor, preload, number of pads, and pad loading.

Prior to any critical speed, unbalance response or stability analyses, accurate tilt-pad bearing data must be known. Very little is available in the literature. An early work compared the performance of a tilt-pad bearing to a journal bearing (15). This paper included a study of load capacity for both on pad and between pad loading. A later paper by the same authors dealt with the effects of bearing preload (16). Experimental stiffness and damping coefficients were presented by Hagg and Sankey (17) for one 4- and one 6-pad bearing. Lund introduced the pad assembly method and presented bearing characteristics for 4-, 5-, 6-, and 12-pad bearings (4). More tilt-pad data may be found in Ref. (18). The bearing data in Ref. (4) and (18) are for the zero preloaded case with a downward load and is inaccurate for two reasons. First, the bearing characteristics include only the effect of the bottom pads (4). These characteristics have increasing error at the higher values of Sommerfeld number (light loads) due to top pad effects (7). Second, the finite difference method was used to solve for the hydrodynamic pressure in calculating the single-pad data (4). In the early 60's, when this data was produced, computer systems were not sophisticated or efficient enough to make it economically feasible to use a large number of nodes. Thus, numerical inaccuracies are also present in the data. Design charts for load capacity and friction loss are shown in Ref. (19) for 3- and 5-pad configurations. Turbulence effects have also been considered. Orcutt (5) presents bearing characteristics for a 4-pad bearing as a function of Reynolds number for 0.0 and 0.5 preloads (offset factor, $a = 0.55$). An experimental study reports velocity profiles and pressure distributions for turbulent flow under tilt pad bearings using air as the working fluid (20).

Presently, the effects of bearing preload, offset and pad loading on the stiffness and damping coefficients of a tilt-pad bearing are not fully investigated in the literature. Tilt-pad bearing data for different geometric designs must be available to the manufacturers and users of high speed, high performance turbo machinery. Without reliable bearing data, proper bearing design can only be guesswork. This paper presents stiffness and damping curves for the five-pad tilt-pad bearing. The five-pad configuration was chosen since it is the most popular in industrial application. The effects of changing preload, offset and pad loading are illustrated.

TILT-PAD BEARING CHARACTERISTICS

The bearing characteristics for a 5-pad tilt-pad bearing were determined using the pad assembly method (4) (see Appendix 1). The hydrodynamic pressures for the single-pad data were calculated using the finite element matrix formulation of Ref. (21). The small effects of pad inertia and pivot friction (4) have been neglected. It was found that the top pads do, indeed, contribute to the tilt-pad bearing damping and, in some cases, the bearing stiffness (Appendix 1). Note that in all tilt-pad bearing data presented here (Figs. 2-6, 11-16) the horizontal and vertical damping curves approach each other at high Sommerfeld numbers (low eccentricities). At these high Sommerfeld numbers, the eccentricity should approach zero where the bearing characteristics will be symmetrical. The bearing data of Refs. (4) and (18) do not show this trend for the bearing damping at high Sommerfeld numbers due to neglecting the damping contribution of the top pads. The bearing data presented here was calculated on a CDC 6400 computer where it was economically feasible to use a large number of nodes in the finite element (up to 5×49 to cover one axial half of a single pad). Thus, numerical inaccuracies have been kept to a minimum. Furthermore, a Newton/Raphson iterative scheme was used to determine the equilibrium position of the single pad. This iterative scheme, due to its fast convergence, permitted the determination of an accurate equilibrium position (22). Small numerical perturbations about this position in displacement and velocity determined the characteristics of the single pad. Since the equilibrium position has been determined to a fine degree of accuracy (error criterion for the normalized hydrodynamic load is 1.0×10^{-3}), the stiffness and damping coefficients should, therefore, be more accurate than previous methods of determining equilibrium. Appendix 2 contains an accuracy study varying the number of axial and circumferential nodes for a 60-degree single pad.

For this analysis, a pad arc length of $\chi = 60$ degrees was considered with a length to diameter ratio of L/D = 0.5. Bearing characteristics for other length to diameter ratios (L/D = 1.0, 1.5) for the 5-pad bearing are presented in Appendix 3. Also contained in Appendix 3 is the single-pad data used to construct the full tilt-pad bearing data.

A 5-pad bearing is shown in Fig. 1 with on-pad loading. Figure 2 shows dimensionless stiffness and damping coefficients vs Sommerfeld number for a tilt-pad bearing with on-pad loading and offset factor, $\alpha = 0.5$ (centrally pivoted). These curves show the effect of changing the bearing preload, m_b, from 0.0 to 0.5. A dramatic increase in the X-direction stiffness is evident for the $m_b = 0.5$ bearing. This increase in $\overline{K}_{xx}$ ranges from a factor of 10 at low Sommerfeld numbers to a factor of 50 for high Sommerfeld numbers. A corresponding increase in $\overline{C}_{xx}$ is seen but only by a factor of 4. The 0.5 preload also increases the Y-direction stiffness and damping at high Sommerfeld numbers.

Figure 3 compares on- and between-pad loading for the $\alpha = 0.5$, $m_b = 0.0$ case. The characteristics of these two bearings approach each other for high Sommerfeld numbers. For low Sommerfeld numbers, the X-direction stiffness and damping are increased up to a factor of 40 and 20, respectively, for the between-pad loading. This plot shows that these two bearings should perform similarly for low loads and/or high speeds.

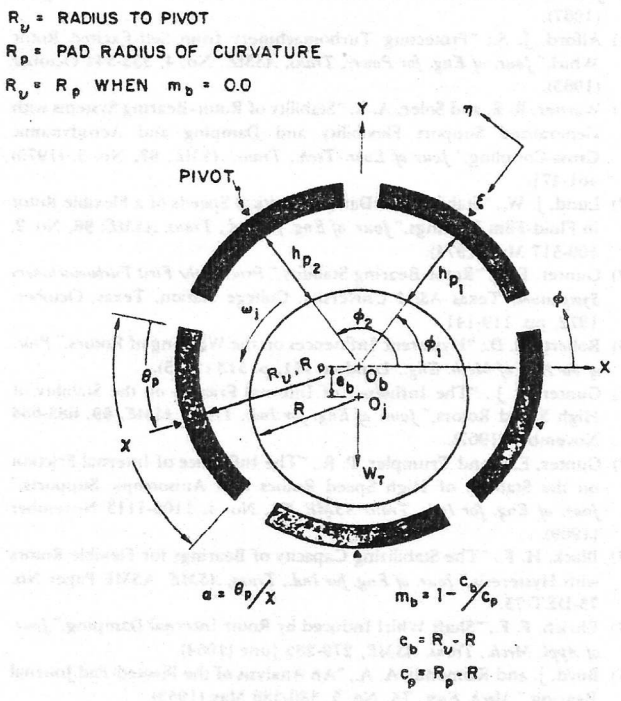

Fig. 1—Tilt-pad bearing schematic

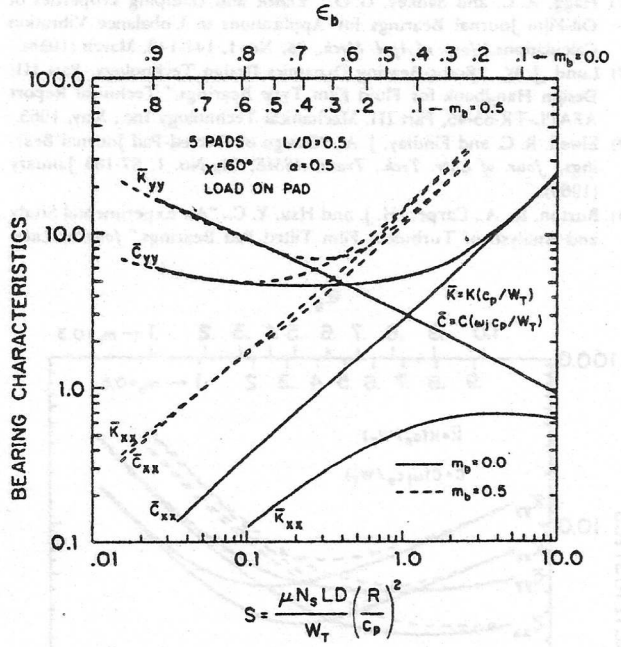

Fig. 2—Tilt-pad bearing characteristics—The effect of changing the bearing preload from m_b = 0.0 to m_b = 0.5 for the load on pad, centrally-pivoted bearing.

The zero preload, load on pad bearing is shown in Fig. 4 for $\alpha = 0.5$ and $\alpha = 0.55$. The biggest change is the large increase in X-direction stiffness over the full range of Sommerfeld numbers for the $\alpha = 0.55$ bearing. Another interesting trend is that the X- and Y-direction stiffness coefficients approach each other at a lower Sommerfeld number for the $\alpha = 0.55$ bearing. The same type of occurence is seen in Fig. 2 for the $m_b = 0.5$ case. This indicates that the $m_b = 0.0$, $\alpha = 0.5$ bearing retains its stiffness asymmetry for a higher range of Sommerfeld numbers, thereby possibly enhancing machine stability (*12*).

Figure 5 shows the bearing characteristics for a 0.3 preload, load on pad bearing with $\alpha = 0.5$ and 0.55 offsets. Figure 6 considers a centrally pivoted ($\alpha = 0.5$), load between pad bearing with preload values of 0.3 and 0.5. Both plots shows that increasing the preload and increasing the offset factor increases the bearing characteristics over the high Sommerfeld number range.

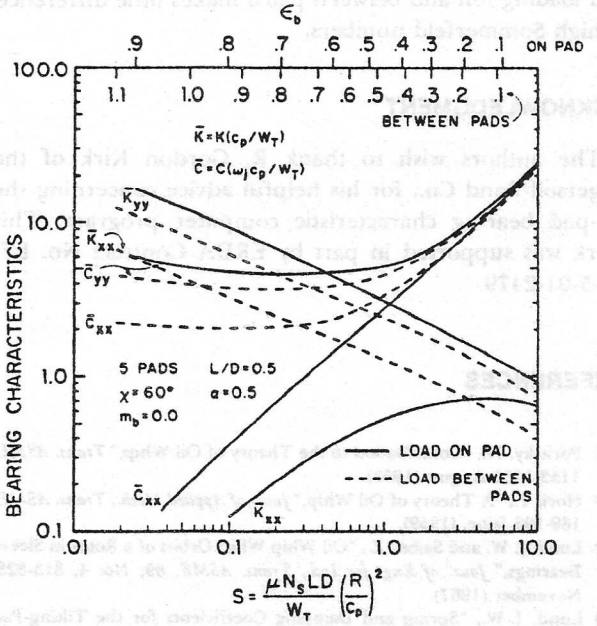

Fig. 3—Tilt-pad bearing characteristics—The effect of changing pad loading from load on pad to load between pads for the zero preload, centrally-pivoted bearing.

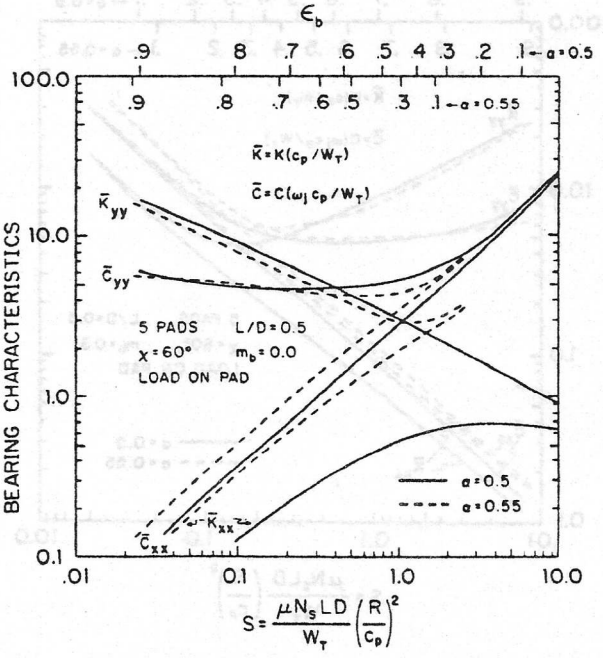

Fig. 4—Tilt-pad bearing characteristics—The effect of changing offset factor from α = 0.5 (centrally pivoted) to α = 0.55 for the load on pad, zero preload bearing.

CONCLUSIONS

Reliable tilt-pad bearing data is presented in Section 2 and Appendix 3 for the 5-pad configurations using the finite element matrix approach and the pad assembly method. The top, unloaded pads do contribute to damping in all cases and to stiffness only when the pads are not centrally pivoted ($\alpha = 0.5$). The effect of increasing bearing preload is to increase the bearing stiffness and to eliminate stiffness asymmetry at high Sommerfeld numbers. The effect of increasing bearing offset is similar but less drastic. Pad loading (on and between pads) makes little difference at high Sommerfeld numbers.

ACKNOWLEDGMENT

The authors wish to thank R. Gordon Kirk of the Ingersoll-Rand Co., for his helpful advice concerning the tilt-pad bearing characteristic computer program. This work was supported in part by ERDA Contract No. EF-76-5-01-2479.

REFERENCES

(1) Poritsky, H., "Contribution to the Theory of Oil Whip," *Trans. ASME*, 1153-1161 August (1953).

(2) Hori, Y., "A Theory of Oil Whip," *Jour. of Applied Mech., Trans. ASME*, 189-198 June, (1959).

(3) Lund, J. W. and Saibel, E., "Oil Whip Whirl Orbits of a Rotor in Sleeve Bearings," *Jour. of Eng. for Ind., Trans. ASME*, **89**, No. 4, 813-823, November (1967).

(4) Lund, J. W., "Spring and Damping Coefficients for the Tilting-Pad Journal Bearing," *ASLE Trans.*, **7**, No. 4, 342-352 (1964).

(5) Orcutt, F. K., "The Steady State and Dynamic Characteristics of the Tilting Pad Journal Bearing in Laminar and Turbulent Flow Regimes," *Jour. of Lubr. Tech., Trans. ASME*, Series F, **89**, No. 3, 392-404 July, (1967).

(6) Alford, J. S., "Protecting Turbomachinery from Self-Excited Rotor Whirl," *Jour. of Eng. for Power, Trans. ASME*, No. 4, 333-344 October (1965).

(7) Warner, R. E. and Soler, A. I., "Stability of Rotor-Bearing Systems with Generalized Support Flexibility and Damping and Aerodynamic Cross-Coupling," *Jour of Lubr. Tech., Trans. ASME*, **97**, No. 3, (1975) 461-471.

(8) Lund, J. W., "Stability and Damped Critical Speeds of a Flexible Rotor in Fluid-Film Bearings," *Jour. of Eng. for Ind., Trans. ASME*, **96**, No. 2, 509-517 May (1974).

(9) Gunter, E. J., "Rotor-Bearing Stability," *Proc. of the First Turbomachinery Symposium*, Texas A&M University, College Station, Texas, October, 1972, pp. 119-141.

(10) Robertson, D., "Hysteretic Influences on the Whirling of Rotors," *Proc. of the Inst. of Mech. Eng.*, London, **131**, p. 513 (1935).

(11) Gunter, E. J., "The Influence of Internal Friction on the Stability of High Speed Rotors," *Jour. of Eng. for Ind., Trans. ASME*, **89**, 683-688 November (1967).

(12) Gunter, E. J. and Trumpler, P. R., "The Influence of Internal Friction on the Stability of High Speed Rotors with Anisotropic Supports," *Jour. of Eng. for Ind., Trans ASME*, **91**, No. 4, 1105-1113 November (1969).

(13) Black, H. F., "The Stabilizing Capacity of Bearings for Flexible Rotors with Hysteresis," *Jour. of Eng. for Ind., Trans. ASME*, ASME Paper No. 75-DET-75.

(14) Ehrich, F. F., "Shaft Whirl Induced by Rotor Internal Damping," *Jour. of Appl. Mech., Trans. ASME*, 279-283 June (1964).

(15) Boyd, J. and Raimondi, A. A., "An Analysis of the Pivoted-Pad Journal Bearing," *Mech. Eng.*, **75**, No. 5, 380-386 May (1953).

(16) Boyd, J. and Raimondi, A. A., "Clearance Considerations in Pivoted-Pad Journal Bearings," *ASLE Trans.*, **5**, No. 2, 418-426 November (1962).

(17) Hagg, A. C. and Sankey, G. O., "Elastic and Damping Properties of Oil-Film Journal Bearings for Applications to Unbalance Vibration Calculations," *Jour. of Appl. Mech.*, **25**, No. 1, 141-143, March (1958).

(18) Lund, J. W., "Rotor-Bearing Dynamics Design Technology, Part III: Design Handbook for Fluid Film Type Bearings," Technical Report AFAPL-TR-65-45, Part III, Mechanical Technology Inc., May, 1965.

(19) Elwell, R. C. and Findlay, J. A., "Design of Pivoted-Pad Journal Bearings," *Jour. of Lubr. Tech., Trans. ASME*, **91**, No. 1, 87-103 January (1969).

(20) Burton, R. A., Carper, H. J. and Hsu, Y. C., "An Experimental Study and Analysis of Turbulent Film Tilted Pad Bearings," *Jour. of Lubr.*

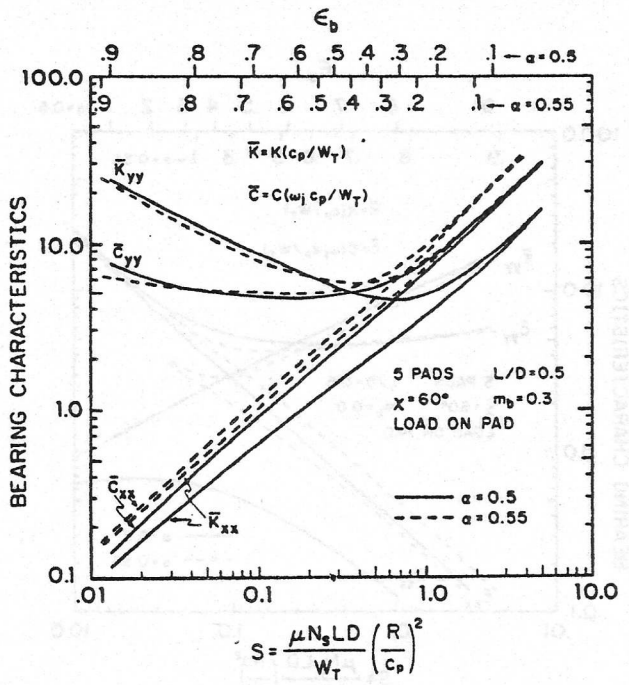

Fig. 5—Tilt-pad bearing characteristics—The effect of changing offset factor from $\alpha = 0.5$ (centrally pivoted) to $\alpha = 0.55$ for the load on pad, $m_b = 0.3$ bearing.

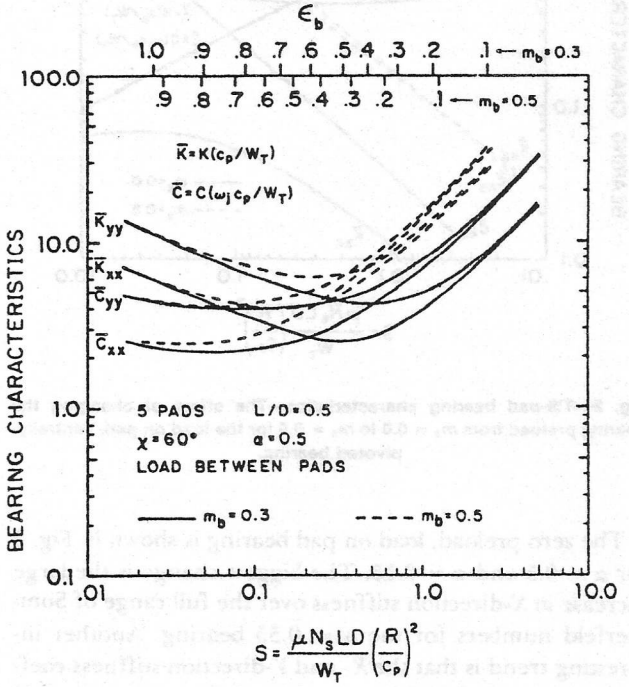

Fig. 6—Tilt-pad bearing characteristics—The effect of increasing preload from $m_b = 0.3$ to $m_b = 0.5$ for the load between pads, centrally-pivoted bearing.

Tech., Trans. ASME, Series F, **96**, No. 1, 168-173 January (1974).

(*21*) Allaire, P. E., Nicholas, J. C. and Gunter, E. J., "Systems of Finite Elements for Finite Bearings," *Jour. of Lubr. Tech., Trans. ASME*, **99**, No. 2, 187-197 April (1977).

(*22*) Eierman, R. G., "Stability Analysis and Transient Motion of Axial Groove, Multilobe and Tilting Pad Bearings," MS Thesis, University of Virginia, August, 1976.

(*23*) Carnahan, B., Luther, H. A. and Wilkes, J. O., *Applied Numerical Methods*, Wiley, New York, 1969, pp. 27-34.

APPENDIX 1

PAD ASSEMBLY METHOD—TILT-PAD BEARINGS

For liquid lubricated bearings, the pad inertia may be neglected (*4*). With symmetry about the Y-axis, the stiffness and damping coefficients for the full tilt-pad bearing in dimensionless form are (*4*)

$$\overline{K}_{xx} = \sum_{i=1}^{n_p} (\overline{K}'_{\xi\xi} \cos^2\Psi)_i \qquad [1]$$

$$\overline{K}_{yy} = \sum_{i=1}^{n_p} (\overline{K}'_{\xi\xi} \sin^2\phi)_i \qquad [2]$$

$$\overline{C}_{xx} = \sum_{i=1}^{n_p} (\overline{C}'_{\xi\xi} \cos^2\phi)_i \qquad [3]$$

$$\overline{C}_{yy} = \sum_{i=1}^{n_p} (\overline{C}'_{\xi\xi} \sin^2\phi)_i \qquad [4]$$

$$\overline{K}_{xy} = \overline{K}_{yx} = \overline{C}_{xy} = \overline{C}_{yx} = 0 \qquad [5]$$

where n_p = number of pads

ϕ_i = angle from positive X-axis measured counter-clockwise to the pivot point of the i^{th} pad (Fig. 1)

and

$$\overline{K}_{\xi\xi} = \overline{K}_{\xi\xi} - (\overline{pK}_{\xi\eta} + \overline{qC}_{\xi\eta})\overline{K}_{\eta\xi} - (\overline{qK}_{\xi\eta} - \overline{pC}_{\xi\eta})\overline{C}_{\eta\xi} \qquad [6]$$

$$\overline{C}'_{\xi\xi} = \overline{C}_{\xi\xi} - (\overline{pK}_{\xi\eta} + \overline{qC}_{\xi\eta})\overline{C}_{\eta\xi} + (\overline{qK}_{\xi\eta} - \overline{pC}_{\xi\eta})\overline{K}_{\eta\xi} \qquad [7]$$

with

$$P = \frac{\overline{K}_{\eta\eta}}{\overline{K}_{\eta\eta}^2 + \overline{C}_{\eta\eta}^2} \qquad [8]$$

$$q = \frac{\overline{C}_{\eta\eta}}{\overline{K}_{\eta\eta}^2 + \overline{C}_{\eta\eta}^2} \qquad [9]$$

The quantities on the right hand side of equations [6] through [9] ($\overline{K}_{\xi\xi}$, $\overline{K}_{\xi\eta}$, $\overline{K}_{\eta\xi}$, $\overline{K}_{\eta\eta}$, $\overline{C}_{\xi\xi}$, $\overline{C}_{\xi\eta}$, $\overline{C}_{\eta\xi}$, $\overline{C}_{\eta\eta}$) are the dimensionless fixed-pad coefficients. Appendix 2 contains an accuracy study that demonstrates the changes in these fixed pad coefficients for a 60 degree pad as a function of varying the number of axial and circumferencial nodes. These coefficients are calculated by loading up a single fixed-pad, obtaining an equilibrium position and perturbating about the equilibrium position to determine the fixed-pad coefficients (see Fig. 7). Then the pads dynamic coefficients, $\overline{K}'_{\xi\xi}$ and $\overline{C}'_{\xi\xi}$, are calculated using Eq. [6] through [9]. The other 6 dynamic coefficients are zero for no pad inertia. These 2 dynamic coefficients along with the fixed-pad Sommerfeld number, S are stored as a function of the pads dimensionless pivot film thickness, $\overline{h}_p$ where

$$\overline{h}_p = h_p / c_p$$

and

c_p = pad radial clearance

h_p = pivot film thickness (Figs. 1, 7)

Plots of single pad dynamic coefficients as a function of S and $\overline{h}_p$ may be found in Appendix 3, Figs. 8 through 10.

To determine the bearing characteristics of the full tilt-pad bearing, a bearing eccentricity ratio, ϵ_b is chosen where

$$\epsilon_b = \frac{e_b}{c_b} \qquad [10]$$

and

c_b = tilt-pad bearing assembled radial clearance in line with a pivot*

e_b = tilt-pad bearing eccentricity (Fig. 1)

Secondly, the dimensionless pivot film thickness is calculated for the i^{th} pad, $\overline{h}_{Pi}$. Next $\overline{K}'_{\xi\xi_i}$, $\overline{C}'_{\xi\xi_i}$ and S_i are determined for the corresponding h_{Pi} value using a 4-point Lagrangian interpolation (*23*). This is repeated for each pad. Equations [1] through [4] are then used to determine the dimensionless stiffness and damping coefficients for the full tilt-pad bearing. Now, the dimensionless load must be calculated for each pad

$$\overline{W}_{x_i} = \overline{S}_i^{-1} \cos\phi_i \qquad [11]$$

$$\overline{W}_{y_i} = -S_i^{-1} \sin\phi_i \qquad [12]$$

*The bearing clearance c_b can be thought of as the largest shaft (shaft radius = $R + c_b$) which can be placed in the bearing after it is assembled. For a bearing with zero preload, the shaft with radius $R + c_b$ would be in contact with the pad at all points. For a bearing with nonzero preload, shaft-pad contact will occur only along the pivot line.

III-55

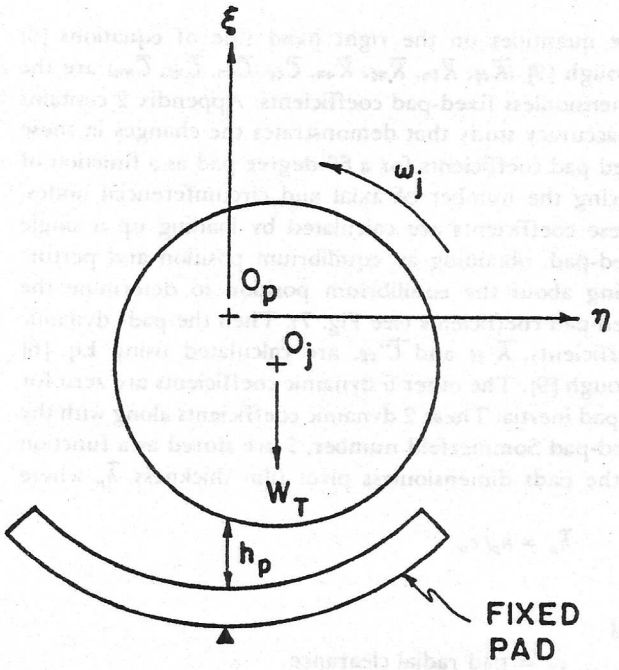

Fig. 7—Single-pad schematic

For the full bearing

$$\overline{W}_x = \sum_{i=1}^{n_p} \overline{W}_{x_i} \qquad [13]$$

$$\overline{W}_y = \sum_{i=1}^{n_p} \overline{W}_{y_i} \qquad [14]$$

The Sommerfeld number for the tilt-pad bearing is

$$S = \overline{W}_y^{-1} \qquad [15]$$

and

$$\overline{W}_x = 0$$

The top pads of a zero preloaded tilt-pad bearing have dimensionless pivot film thicknesses, $\overline{h}_{P\,i}$, greater than 1.0 for the case of a horizontal shaft with a downward load. However, these pads still contribute to the bearing damping. That is, even if $\overline{h}_{p\,i} > 1.0$, $\overline{C}_{\xi\xi\,i}$ is nonzero and positive and contributes to $\overline{C}_{xx}$ and $\overline{C}_{yy}$ in Eqs. [3] and [4]. On the other hand, $\overline{K}'_{\xi\xi\,i}$ approaches zero as $\overline{h}_{p\,i}$ approachs 1.0. Thus, it is set to zero for $\overline{h}_{p\,i} > 1.0$. An exception is for $\alpha = 0.55$. In this case, $\overline{K}'_{\xi\xi\,i}$ has nonzero, positive values for $\overline{h}_{p\,i} > 1.0$. These trends may be observed in Appendix 3, Figs. 8 through 10.

Note that the transformation equations between the X, Y system and the ξ,η system are

$$\begin{Bmatrix} \xi \\ \eta \end{Bmatrix} = - \begin{bmatrix} \cos\phi & \sin\phi \\ -\sin\phi & \cos\phi \end{bmatrix} \begin{Bmatrix} X \\ Y \end{Bmatrix} \qquad [16]$$

Also, the assumption of symmetry about the Y-axis holds for all load on pad (load on pivot) and load between pad (load between pivot) bearings. Finally, the transformation from fixed-pad data to dynamic-pad data, Eqs. [6] [9], may be viewed as an adjustment in the fixed-pad data to allow the pad to pitch so that the load, W_T will pass through the pivot point.

APPENDIX 2

ACCURACY STUDY—60-DEGREE SINGLE-PAD

Table 1 contains fixed-pad stiffness coefficients and eccentricity ratio as a function of the Sommerfeld number for various combinations of axial and circumferential nodes. Table 2 shows the variance in the fixed-pad damping coefficients and attitude angle for the same study. The percent largest error is also indicated. For each Sommerfeld number, the equilibrium position is first obtained using a Newton-Raphson iterative scheme (*22*). The fixed-pad stiffness and damping coefficients are obtained by displacement and velocity perturbations about the equilibrium

TABLE 1—FIXED-PAD STIFFNESS COEFFICIENTS AND ECCENTRICITY RATIO AS A FUNCTION OF SOMMERFELD NUMBER FOR VARIOUS NODE COMBINATIONS (AXIAL x CIRCUMFERENTIAL)- L/D = 0.5, $\chi = 60°$, $\alpha = 0.5$.

S SOMMERFELD NUMBER	NODES (3 × 13)	NODES (4 × 13)	NODES (4 × 21)	NODES (4 × 31)	NODES (5 × 49)	% LARGEST ERROR
0.101	0.846	0.841	0.840	0.840	0.839	0.8
0.318	0.725	0.719	0.718	0.718	0.716	1.2
1.01	0.553	0.545	0.544	0.544	0.542	2.0 ϵ_b
3.18	0.339	0.331	0.330	0.330	0.327	3.7
10.1	0.147	0.141	0.141	0.141	0.139	5.8
0.101	0.984	0.991	0.989	0.981	0.972	2.0
0.318	0.682	0.675	0.667	0.665	0.661	3.2
1.01	0.462	0.459	0.455	0.454	0.452	2.2 $\overline{K}_{\eta\eta}$
3.18	0.332	0.331	0.329	0.328	0.328	1.2
10.1	0.270	0.271	0.270	0.270	0.270	0.4
0.101	−0.138	−0.118	−0.103	−0.104	−0.103	34.0
0.318	−0.028	−0.024	−0.022	−0.022	−0.020	13.0
1.01	0.039	0.043	0.044	0.045	0.046	15.2 $\overline{K}_{\eta\xi}$
3.18	0.100	0.105	0.107	0.107	0.110	9.1
10.1	0.216	0.228	0.233	0.234	0.240	10.0
0.101	−5.56	−5.53	−5.53	−5.52	−5.49	1.3
0.318	−4.59	−4.55	−4.50	−4.49	−4.47	2.7
1.01	−4.22	−4.20	−4.16	−4.14	−4.13	2.2 $\overline{K}_{\xi\eta}$
3.18	−4.76	−4.80	−4.75	−4.73	−4.74	1.3
10.1	−7.95	−8.18	−8.14	−8.11	−8.19	2.9
0.101	11.2	11.3	11.2	11.2	11.2	0.9
0.318	7.45	7.33	7.31	7.30	7.25	2.8
1.01	5.02	4.94	4.93	4.92	4.89	2.7 $\overline{K}_{\xi\xi}$
3.18	3.59	3.55	3.54	3.54	3.52	2.0
10.1	2.92	2.90	2.90	2.90	2.89	1.0

TABLE 2—FIXED-PAD DAMPING COEFFICIENTS AND ATTITUDE ANGLE AS A FUNCTION OF SOMMERFELD NUMBER FOR VARIOUS NODE COMBINATIONS (AXIAL x CIRCUMFERENTIAL) L/D = 0.5, χ = 60°, α = 0.5.

S SOMMERFELD NUMBER	NODES (3 × 13)	NODES (4 × 13)	NODES (4 × 21)	NODES (4 × 31)	NODES (5 × 49)	% LARGEST ERROR
0.101	17.4°	17.6°	18.0°	18.1°	18.2°	4.4
0.318	21.2°	21.6°	22.0°	22.1°	22.3°	4.9
1.01	27.9°	28.4°	28.9°	29.0°	19.3°	4.8 Ψ
3.18	39.8°	40.6°	41.2°	41.4°	41.8°	4.8
10.1	59.7°	60.8°	61.4°	61.5°	62.0°	3.7
0.101	0.439	0.454	0.466	0.464	0.460	4.6
0.318	0.326	0.327	0.329	0.329	0.330	1.2
1.01	0.271	0.274	0.276	0.277	0.279	2.9 $\bar{C}_{\eta\eta}$
3.18	0.288	0.296	0.299	0.300	0.304	5.3
10.1	0.469	0.491	0.500	0.502	0.513	8.6
0.101	−1.40	−1.42	−1.43	−1.42	−1.40	2.1
0.318	−0.836	−0.823	−0.812	−0.809	−0.803	4.1
1.01	−0.509	−0.503	−0.499	−0.498	−0.495	2.8
3.18	−0.344	−0.343	−0.340	−0.340	−0.339	1.5 $\bar{C}_{\eta\xi}$
10.1	−0.272	−0.273	−0.272	−0.272	−0.272	0.4
0.101	−1.38	−1.39	−1.42	−1.42	−1.40	1.4
0.318	−0.804	−0.794	−0.801	−0.803	−0.801	0.9
1.01	−0.491	−0.487	−0.492	−0.494	−0.494	1.4 $\bar{C}_{\xi\eta}$
3.18	−0.333	−0.332	−0.336	−0.338	−0.338	1.8
10.1	−0.263	−0.265	−0.269	−0.270	−0.271	3.0
0.101	12.3	12.2	12.1	12.0	11.9	3.4
0.318	9.67	9.55	9.41	9.37	9.31	3.9
1.01	8.64	8.59	8.48	8.45	8.41	2.7 $\bar{C}_{\xi\xi}$
3.18	9.60	9.66	9.57	9.54	9.55	0.5
10.1	15.9	16.4	16.3	16.3	16.4	3.0
Compile time	27	27	27	27	27	
Execution time	28	37	53	66	129	
CDC 6400 – 5 values of S						

position. For each Sommerfeld case, 5 different node combinations are used ranging from 3 × 13 nodes to 5 × 49 nodes (axial × circumferential). Due to symmetry, only one axial half of the pad is analyzed. Thus, the number of axial nodes corresponds to one half of the pad. The percent largest error is usually the error between the 3 × 13 case and the 5 × 49 case. The most sensitive parameter is $\bar{K}_{\eta\xi}$ where the percent errors are the highest. Note that the error between the 4 × 31 case and the 5 × 49 case is very small for all parameters. However, the 5 × 49 case requires almost twice the execution time (Table 2). For this reason, 4 × 31 nodes are normally used in this study to evaluate the fixed-pad coefficients.

APPENDIX 3

PAD AND TILT-PAD BEARING CHARACTERISTICS

The single-pad dynamic data used to construct the tilt-pad bearing data presented in Section 2 is shown in Fig. 8. Pad data for length to diameter ratios of L/D = 1.0 and 1.5 is plotted in Figs. 9 and 10, respectively. Figures 11, 12 and 13 contain tilt-pad bearing data for L/D = 1.0. Figures 14, 15 and 16 consider the L/D = 1.5 case. Three different preloads are presented (m_b = 0.0, 0.3, 0.5) along with the two types of pad loading (on pad and between pad) for the centrally pivoted case (α = 0.5). For all plots shown here, the 5-pad bearing is considered with a pad arc length of χ = 60 degrees.

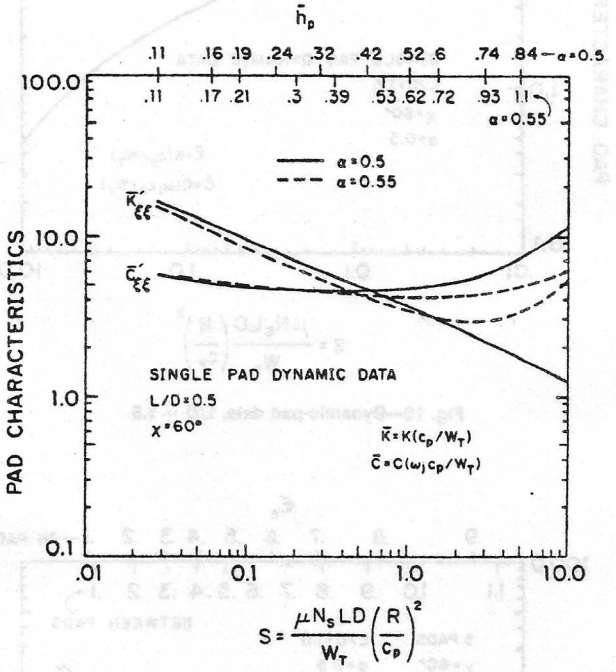

Fig. 8—Dynamic-pad data, L/D = 0.5

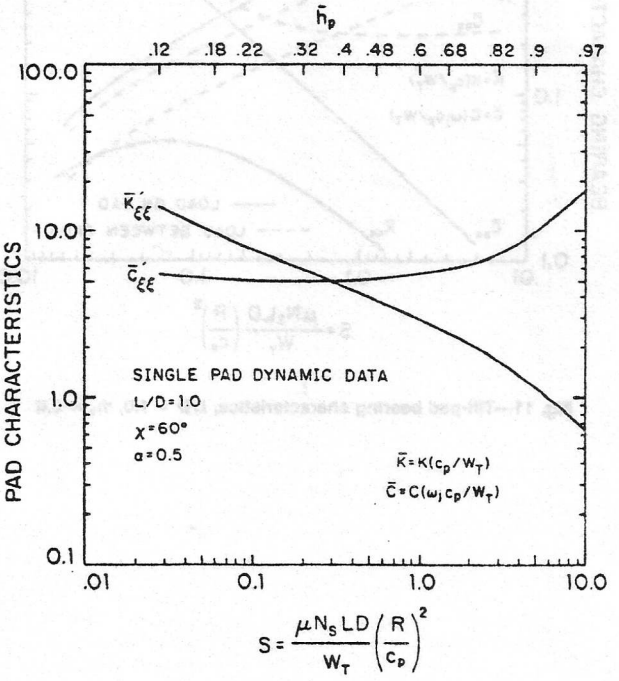

Fig. 9—Dynamic-pad data, L/D = 1.0

III - 57

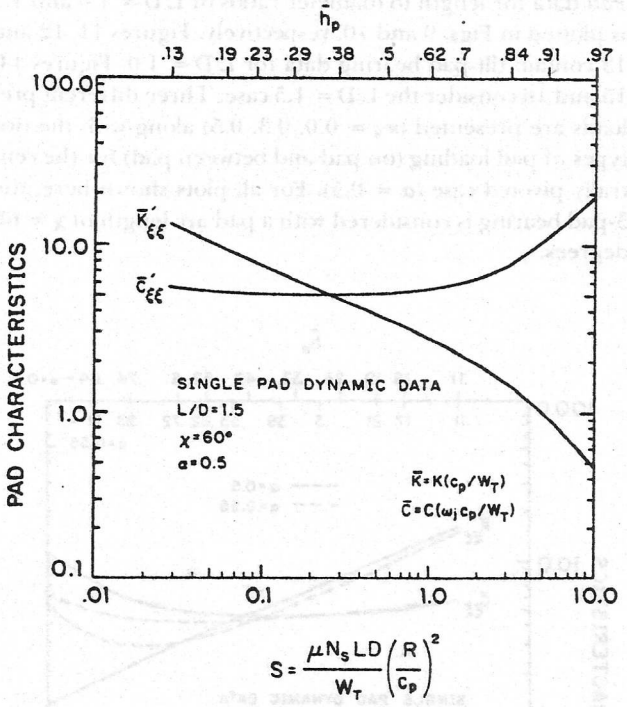

Fig. 10—Dynamic-pad data, L/D = 1.5

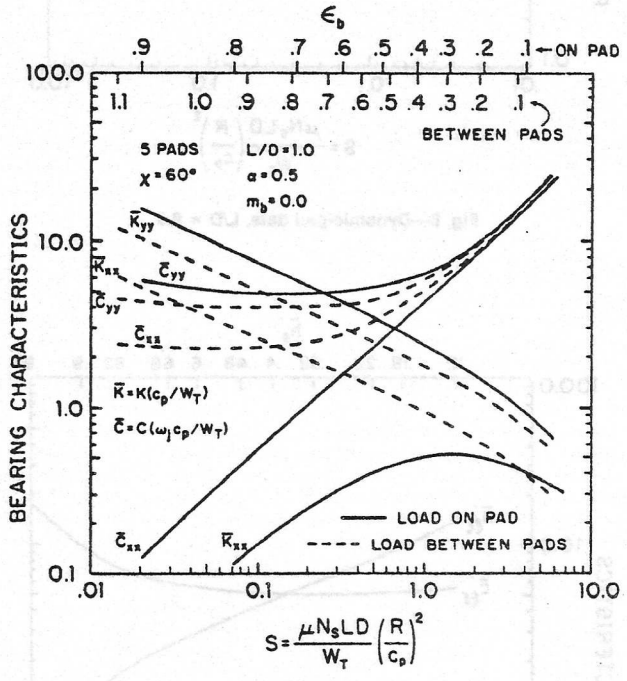

Fig. 11—Tilt-pad bearing characteristics, L/D = 1.0, m_b = 0.0

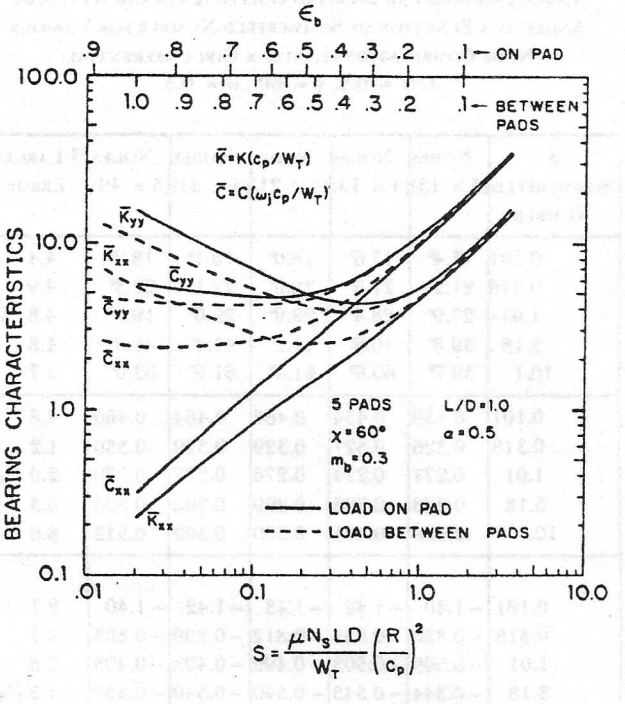

Fig. 12—Tilt-pad bearing characteristics, L/D = 1.0, m_b = 0.3

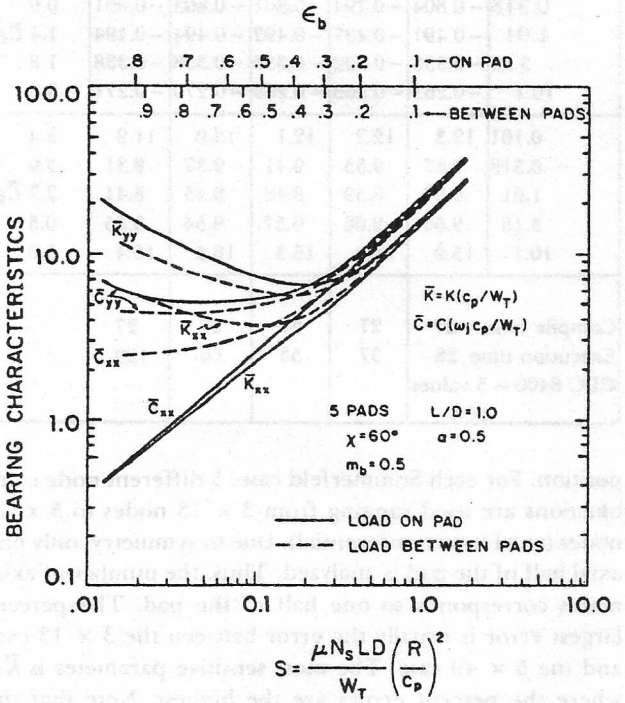

Fig. 13—Tilt-pad bearing characteristics, L/D = 1.0, m_b = 0.5

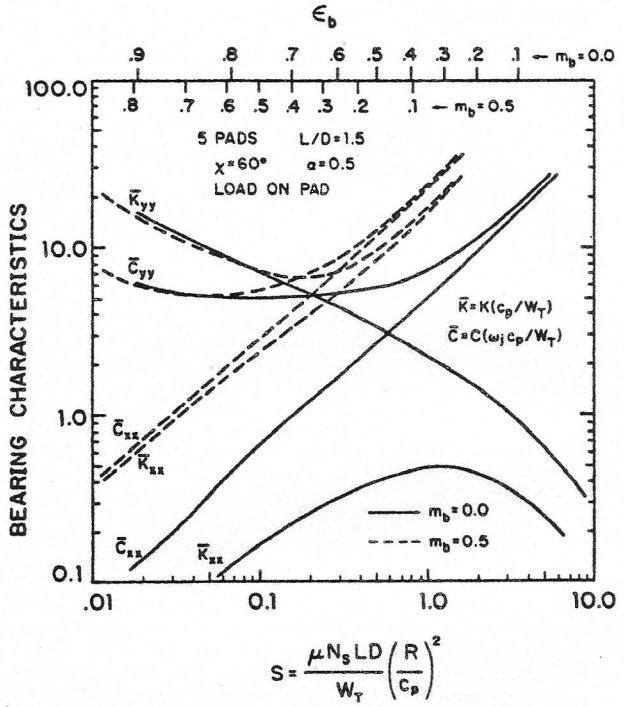

Fig. 14—Tilt-pad bearing characteristics, L/D = 1.5, m_b = 0.0, 0.5, load on pad.

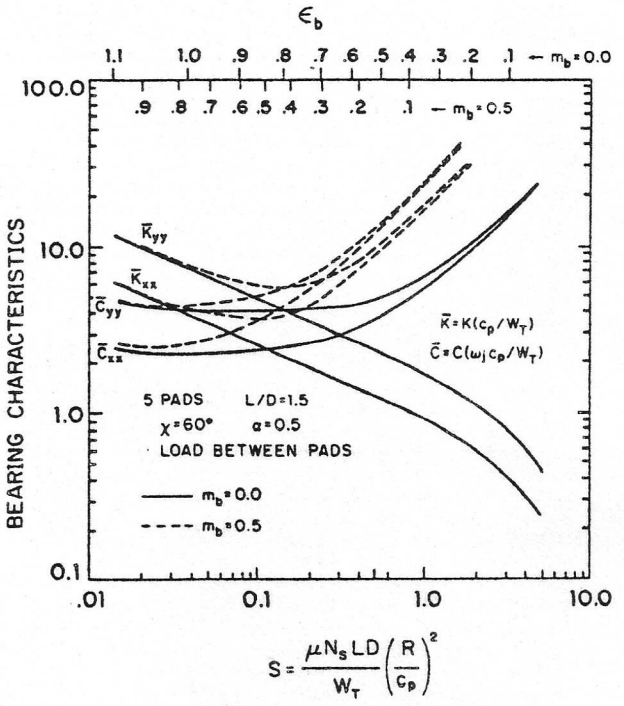

Fig. 15—Tilt-pad bearing characteristics, L/D = 1.5, m_b = 0.0, 0.5, load between pads.

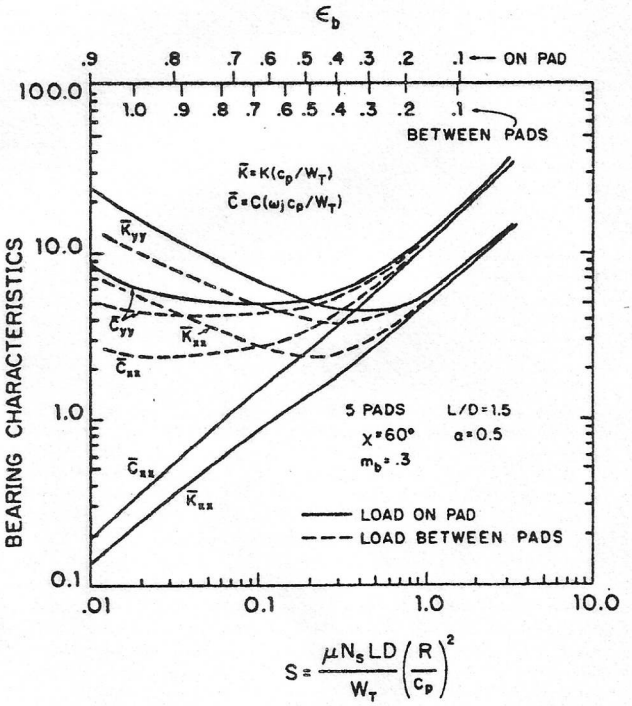

Fig. 16—Tilt-pad bearing characteristics, L/D = 1.5, m_b = 0.3

Presented at the ASLE/ASME Lubrication Conference, Kansas City, Missouri, October 3-5, 1977: This paper is the literary property of the American Society of Lubrication Engineers. The Press may summarize freely from this manuscript after presentation, citing source; however, publication of material constituting more than 20 percent of the manuscript shall be construed as a violation of the Society's rights and subject to appropriate legal action. Manuscripts not to be published by the Society will be released in writing for publication by other sources. Statements and opinions advanced in papers are understood to be individual expressions of the author(s) and not those of the American Society of Lubrication Engineers. Discussion of this paper will be accepted at ASLE Headquarters until November 25, 1977.